OPTIMIZATION OF PARTIAL STAINLESS STEEL MELT OXIDATION IN THE EAF

[1,2]Anže BAJŽELJ, [1,2]Jaka BURJA

[1]*Institute of Metals and Technology, Ljubljana, Slovenia, EU, anze.bajzelj@imt.si, jaka.burja@imt.si*

[2]*University of Ljubljana, Faculty of Natural Sciences and Engineering, Department of Materials and Metallurgy, Ljubljana, Slovenia, EU*

https://doi.org/10.37904/metal.2024.4868

Abstract

Stainless steel production typically follows the duplex process, beginning with the electric arc furnace (EAF) and proceeding to the vacuum oxygen decarburizer (VOD) or argon oxygen decarburizer (AOD). The EAF's role is to melt the charge and heat it up for further processing, reducing tap-to-tap times through partial oxidation. However, this partial oxidation in the EAF leads to chromium losses as oxygen interacts with the high chromium steel melt. To address this issue, parameters affecting chromium burn-off have been identified and presented. A primary challenge in EAF steel production with elevated chromium content is to lower carbon levels while maximizing chromium yield in the melt. Unlike VOD and AOD processes, which permit low carbon and high chromium levels through vacuum or argon blowing, the EAF provides limited protection, mainly through silicon. At higher temperatures, carbon oxidation predominates, hence it is important to limit oxygen input into the system in the initial stages, while “protecting” the chromium with silicon. During the oxidation phase of the steel melt, carbon content decreases; however, attention must be paid to ensure that the concentration is not too low, as this increases chromium activity in the melt, leading to more intense oxidation. A practical model, derived from thermodynamic calculations, has been developed to guide carbon, chromium, and other element oxidation during scrap melting. This model, validated through industrial trials, aids in optimizing steel melt oxidation to minimize chromium losses effectively.

Keywords: EAF, stainless steel scrap, carbon oxidation, chromium oxidation, thermodynamics

1. INTRODUCTION

In the production of stainless steels, particular attention must be paid to reducing chromium losses. Chromium is present in stainless steels at concentrations above 10 wt%. This concentration ensures the corrosion resistance of the steels. Carbon concentrations in stainless steels are typically low, thus decarburization of the melt is necessary during stainless steel production. Usually, the decarburization process occurs in multiple stages. Production of stainless steel starts with the melting of the charge in an electric arc furnace (EAF). Partial decarburization also takes place in the EAF, although this step is limited due to increased chromium loss. Final decarburization occurs during the secondary (ladle) metallurgy in a vacuum oxygen decarburizer (VOD) or argon oxygen decarburizer (AOD). Decarburization in the furnace accelerates the process of stainless steel production, yet chromium losses are greatest at this stage [1–9]. Decarburization of the steel melt is achieved by oxygen blowing, wherein carbon is burnt off. This reaction can be expressed by the following equation:

$$[\mathrm{C}] + [\mathrm{O}] \rightarrow \mathrm{CO}_{(g)} \quad [1]$$

In the melt, there is a high chromium concentration, and the activity of the chromium element is high, leading to the parallel oxidation of the chromium in the furnace. This can be expressed by the following equation:

$$2[Cr] + 3[O] \rightarrow Cr_2O_{3(s)} \quad [2]$$

The reactions of carbon and chromium oxidation can be combined, and a unified expression can be formulated. Based on thermodynamic data, the Gibbs free energy of the reaction was determined, considering the dissolution energies of the element in the iron melt. The Gibbs free energies for chemical reactions were checked in literature sources [2,10–14].

$$3[C] + Cr_2O_{3(s)} \rightarrow 3CO_{(g)} + 2[Cr] \quad [3]$$

$$\Delta G^{\circ}_{(3)} = 748{,}740 - 476.68 \cdot T$$

To present the reduction of chromium oxidation and associated losses, conditions for the reactions of carbon and chromium oxidation were calculated. **Figure 1** illustrates the influence of temperature on the solubility of these elements. With increasing temperature, the solubility of chromium increases, indicating that chromium oxidation is significantly lower at higher oxidation temperatures. Decarburization of the steel melt in the EAF should be performed towards the end when the melt temperature is at its highest.

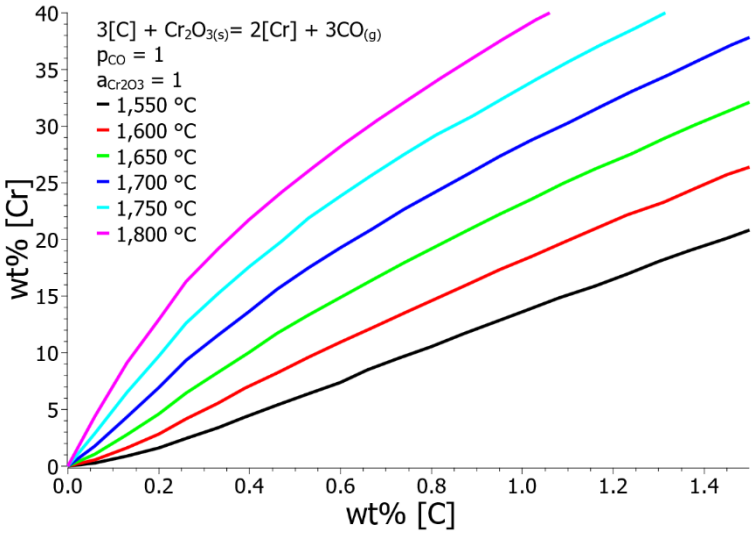

Figure 1 Influence of steel melt temperature on the solubility of carbon and chromium

Figure 2 shows the curves of equilibrium concentrations of C and Cr for different activities of chromium oxide. As the proportion of chromium oxide increases in the slag, its activity increases until it begins to precipitate in solid form and its activity is equal to 1. The equilibrium solubility of chromium in liquid iron is higher at higher activities of chromium oxide, which can be concluded that in the initial stages of melt oxidation, due to the lower activity of chromium oxide, the more intensive oxidation of chromium takes place.

Figure 3 presents the temperature dependence of the Gibbs free energies for the chemical reactions of element oxidation in the steel melt. The oxidation of carbon increases with temperature, while the trend for the other analyzed elements is the opposite. From the diagram, it can be confirmed that decarburization of the stainless steel melt is more suitable at higher temperatures. Additionally, it can be seen from the diagram, that chromium oxidation at low temperatures can be limited by adding silicon or aluminum to the charge. Besides Gibbs free energies, it is necessary to consider the activities of the elements dissolved in liquid melt when calculating oxidation. In stainless steels, there is a high concentration of dissolved chromium in the melt, resulting in a high element activity.

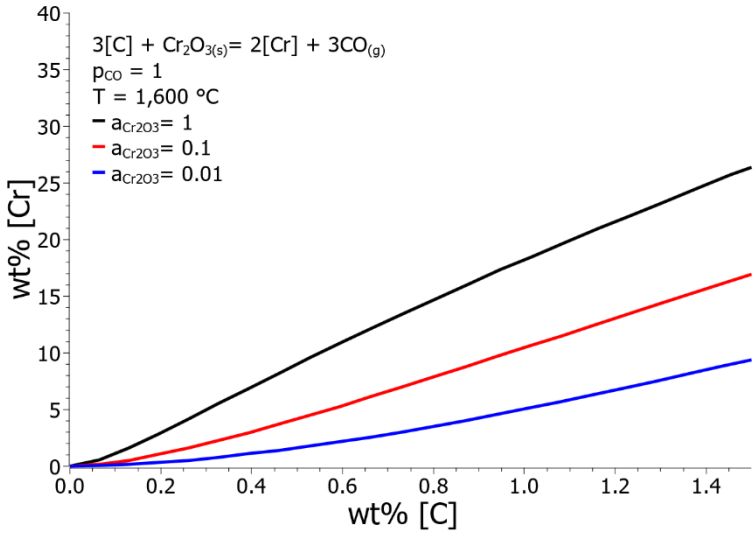

Figure 2 Solubility of chromium and carbon in liquid steel melt at different activity of chromium oxide

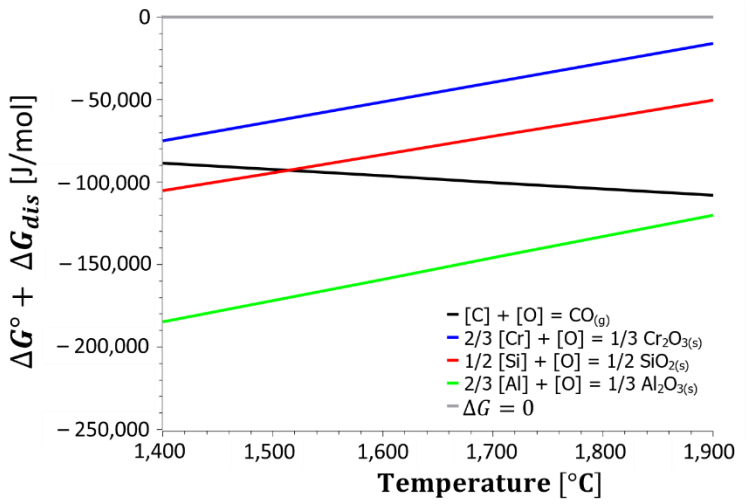

Figure 3 Temperature dependence of Gibbs free energies for oxidation reactions of dissolved elements

The solubility of carbon significantly decreases with a decrease in the pressure of gaseous CO above the steel melt. Lowering the CO pressure intensifies the oxidation of carbon from the melt. Since the CO pressure can not be controlled in the EAF, it is all the more important to be aware that low carbon contents at high chromium activities can only be achieved in VOD or AOD. The diagram in **Figure 4** illustrates the influence of CO pressure above the steel melt on the solubility of carbon and chromium at 1,600 °C.

Data on the oxidation of carbon and chromium in molten stainless steel were collected. Based on thermodynamic data, a simple model was created to calculate the oxidation of carbon, chromium, and other elements. Using this simple model, it is possible to estimate the amount of chromium lost during the decarburization of the melt. The main purpose of the computational model is to identify critical parameters during the decarburization of molten stainless steel and to reduce chromium loss during processing in the EAF.

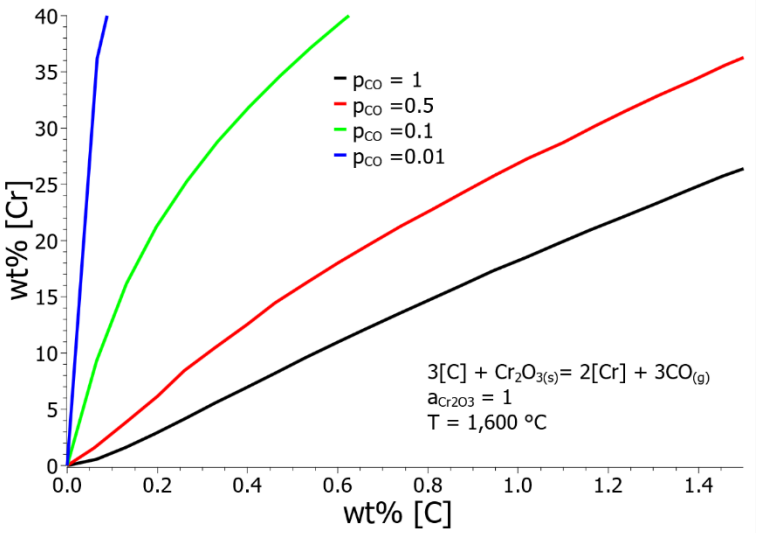

Figure 4 Influence of CO pressure above the steel melt on the solubility of chromium and carbon at 1,600 °C

2. MATERIALS AND METHODS

Based on thermodynamic data, a simple model was developed for calculating the oxidation of elements from the melt of stainless steel. The first step involves determining the initial state of the system, including the weight of the melt in the furnace, its chemical composition, the temperature at the beginning of oxidation, and the desired final content of dissolved carbon. The program calculates the required amount of injected oxygen to achieve the desired composition, taking into account the oxidation of all elements.

Based on the given initial conditions, the activity of elements is determined, followed by oxygen injection into the melt. A small amount of oxygen is introduced into the melt, altering the Gibbs free energy and consequently forming oxides, which are appropriately removed from the melt. This process is repeated with the addition of oxygen to the melt. In each step, before and after oxygen dissolution in the melt and the oxidation process, the chemical composition and temperature of the melt are calculated, and these data are used to determine element oxidation. The calculation process stops when the target composition of the steel melt is reached.

To provide a better approximation of calculating the oxidation of the steel melt to real conditions, several assumptions were included in the calculations, which facilitated the calculation of element oxidation:

- Oxygen blowing into the furnace is carried out through lances, where the concentration of oxygen is high in the immediate vicinity, and the melt temperature is also high, affecting the oxidation conditions. Therefore, the model assumes that oxidation of the melt occurs in 1/3 of the melt weight, while the remaining melt remains unreacted.
- Mixing of the melt in the furnace during oxidation is intensive under real conditions, so the model includes a step of mixing the melt after the prescribed amount of oxygen is injected, resulting in a newly calculated chemical composition, weight, and temperature. These new conditions are then considered in calculating oxidation.
- Heating of the melt during oxidation is intensive, with part of the generated heat being transferred to the slag, part being removed from the system in the form of flue gases, and part being dissipated through water cooling of the furnace walls. The model introduces a factor for heating the melt, which accounts for the described heat dissipation.

The results of calculations from the developed model were verified with measurements from the steel plant. The model was appropriately reviewed and adjusted with the mentioned factors based on real measurements from the steel plant.

3. RESULTS AND DISCUSSION

Figure 5(a–c) graphically shows the calculated quantities of oxidized elements under various decarburization conditions in EAF. The calculations were conducted for a steel melt with 2 wt% C and 15 wt% Cr. In the first scenario, the starting decarburization temperature was set at 1,500 °C, resulting in significant chromium oxidation. With 30 kg of injected oxygen per ton of steel mel, 16 kg of carbon and chromium per ton of steel melt oxidized. As was presented, decarburization of the melt is more favorable at higher temperatures, as shown in the diagram in **Figure 5b**. In this case, decarburization began at 1,650 °C, resulting in the oxidation of 16 kg of carbon and only 9 kg of chromium per ton of steel melt. Besides temperature, the composition of the steel melt plays a significant role in chromium oxidation during decarburization. In this instance, the melt contained 0.5 wt% Si, which significantly reduced chromium oxidation. Here, only 5 kg of chromium per ton of steel melt reacted.

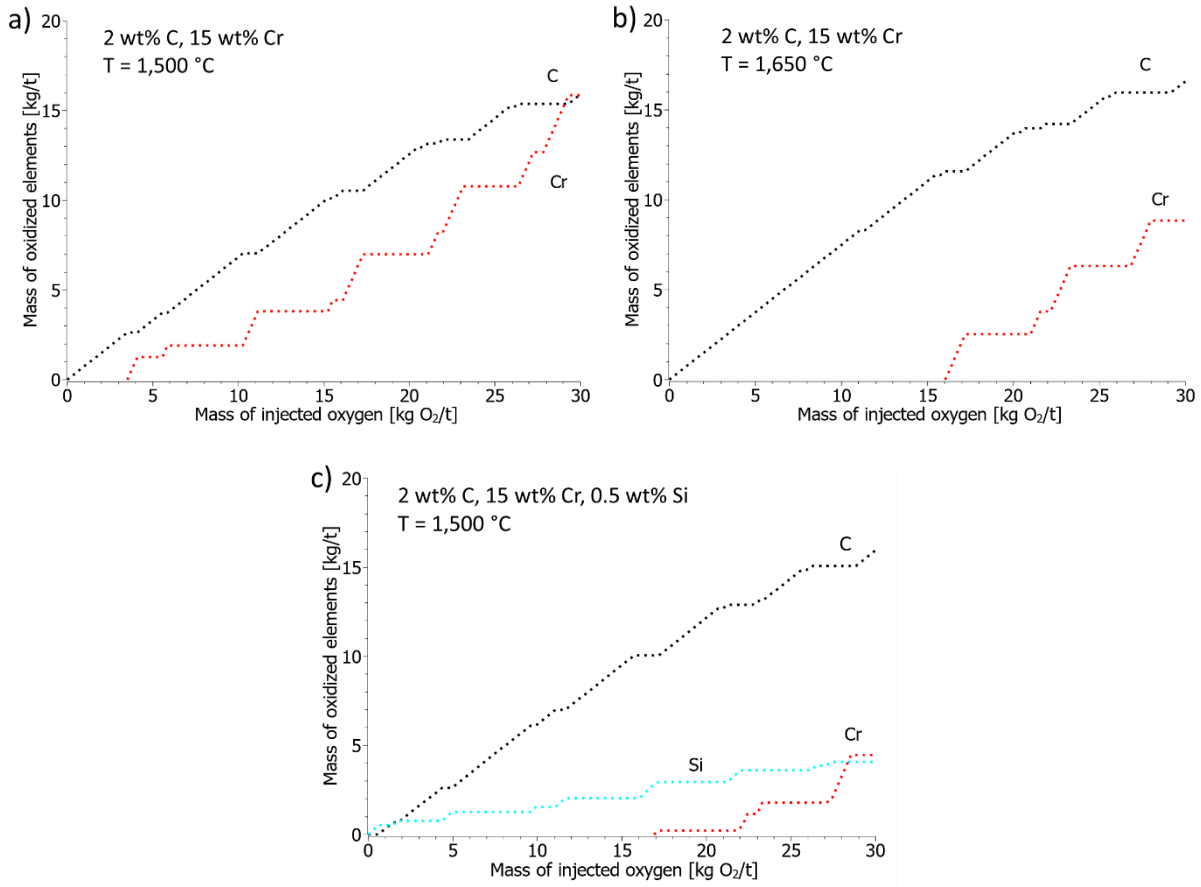

Figure 5 Oxidation of carbon, chromium, and silicon in steel melt with 15 wt% Cr and 2 wt% C. a) Oxidation start temperature 1,500 °C, b) oxidation start temperature 1,650 °C and c) oxidation start temperature 1,500 °C with 0.5 wt% Si

4. CONCLUSION

The research focused on reducing chromium losses during the EAF melting and decarburization process for stainless steel production. Thermodynamic calculations of the oxidation of stainless steel melt were conducted

as part of the research. Chromium losses during stainless steel production are most significant during scarp melting and further treatment of steel melt in the EAF. To address this issue, thermodynamic calculations were performed to describe key parameters in the decarburization step of stainless steel. Increasing the steel melt's temperature increases chromium's solubility, making decarburization more suitable at higher temperatures. The addition of silicon and aluminum to the steel scrap reduces chromium burning, thereby improving its yield. Additionally, a simple model for calculating the oxidation products during decarburization in the EAF was developed, which aids in planning optimal parameters for decarburization.

ACKNOWLEDGEMENTS

Funding was provided by the Slovenian Research Agency ARRS program P2-0050 (C).

REFERENCES

[1] GHOSH, A., CHATTERJEE, A. *Ironmaking and Steelmaking: Theory and Practice*. New Delhi: PHI Learning Private Limited, 2008.

[2] KHO, T.S., SWINBOURNE, D.R., BLANPAIN, B., ARNOUT, S., LANGBERG, D. Understanding Stainless Steelmaking through Computational Thermodynamics Part 1: Electric Arc Furnace Melting. *Trans. Institutions Min. Metall. Sect. C Miner. Process. Extr. Metall*. 2010, vol. 119, pp. 1–8. DOI:10.1179/174328509X431454.

[3] SWINBOURNE, D.R., KHO, T.S., LANGBERG, D., BLANPAIN, B., ARNOUT, S. Understanding Stainless Steelmaking through Computational Thermodynamics Part 2 - VOD Converting. *Trans. Institutions Min. Metall. Sect. C Miner. Process. Extr. Metall*. 2010, vol. 119, pp. 107–115. DOI:10.1179/174328509X481909.

[4] KIRSCHEN, M., JUNG, I.H., HACKL, G. Phase Equilibrium Diagram for Electric Arc Furnace Slag Optimization in High Alloyed Chromium Stainless Steelmaking. *Metals*. 2020, vol. 10, no. 6: 826. DOI:10.3390/met10060826.

[5] HEIKKINEN, E.-P., FABRITIUS, T. Modelling of the Refining Processes in the Production of Ferrochrome and Stainless Steel. In: *Recent Researches in Metallurgical Engineering - From Extraction to Forming*. London: InTechOpen, 2012.

[6] ARH, B., TEHOVNIK, F. The Oxidation and Reduction of Chromium of Stainless Steels in an Eletric Arc Furnace. *Materiali in Tehnologije*. 2007, vol. 41, pp. 203–211.

[7] SANO, N. Reduction of Chromium Oxide in Stainless Steel Slags. In: *Proceedings of the 10th International Ferroalloys Congress*. Cape Town: South African Institute of Mining and Metallurgy, 2004, pp. 670–677.

[8] SWINBOURNE, D.R., KHO, T.S., BLANPAIN, B., ARNOUT, S., LANGBERG, D.E. Understanding Stainless Steelmaking through Computational Thermodynamics: Part 3 - AOD Converting. *Trans. Institutions Min. Metall. Sect. C Miner. Process. Extr. Metall.* 2012, vol. 121, pp. 23–31. DOI:10.1179/1743285511Y.0000000031.

[9] GUO, M., DURINCK, D., JONES, P.T., HEYLEN, G., HENDRICKX, R., BAETEN, R., BLANPAIN, B., WOLLANTS, P. EAF Stainless Steel Refining - Part I: Observational Study on Chromium Recovery in an Eccentric Bottom Tapping Furnace and a Spout Tapping Furnace. *Steel Research International*. 2007, vol. 78, pp. 117–124. DOI:10.1002/srin.200705868.

[10] WANG, H., NZOTT, M.M., TENG, L., SEETHARAMAN, S. Decarburization of Ferrochrome and High Alloy Steels with Optimized Gas and Slag Phases towards Improved Cr Retention. *Journal of Mining and Metallurgy, Section B: Metallurgy*. 2013, vol. 49, pp. 175–181. DOI:10.2298/JMMB120813010W.

[11] BARIN, I. *Thermochemical Data of Pure Substances*. Weinheim: VCH, 1995.

[12] SIGWORTH, G.K., ELLIOTT, J.F. The Thermodynamics of Liquid Dilute Iron Alloys. *Metal Science.* 1974, vol. 8, pp. 298–310. DOI:https://doi.org/10.1179/msc.1974.8.1.298.

[13] CARBONI, M.C., ESPINOSA, D.C.R., TENÓRIO, J.A.S. Reduction of Chromium from Al2O3-CaO-SiO2-CrOx Slags by Carbon Dissolved in Liquid Iron. *ISIJ International*. 2011, vol. 51, pp. 523–529. DOI:10.2355/isijinternational.51.523.

[14] MA, Z., JANKE, D. Thermodynamic Assessment to Chromium Oxidation in the Production of Stainless Steel. *Steel Research*. 2003, vol. 74, pp. 99–103. DOI:10.1002/srin.200300167.